

基于(+)-二对甲基苯甲酰-*D*-酒石酸和铜(II)构筑的 配位聚合物的结构、热稳定性、荧光和染料吸附性质

郑欢 褚衍潇 冯思思* 袁彩霞*

(山西大学分子科学研究所, 化学生物学与分子工程教育部重点实验室, 太原 030006)

摘要: 合成了一种配位聚合物 $[[\text{Cu}(\text{HDTTA})_2(\text{DMF})(\text{H}_2\text{O})]\cdot\text{DMF}\cdot\text{H}_2\text{O}]_n$ (**1**) (D - $\text{H}_2\text{DTTA}=(+)$ -二对甲基苯甲酰- D -酒石酸, $\text{DMF}=N,N$ -二甲基甲酰胺)。通过红外光谱、元素分析、X射线单晶衍射和粉末衍射表征了配合物**1**的结构。配合物**1**沿 a 轴为一维链状结构,在 ab 平面通过弱相互作用形成二维层状结构。热稳定性研究表明配合物**1**的主结构可在197 °C以下稳定存在。在300 nm激发波长条件下,配体的荧光由于和 Cu^{2+} 离子配位而猝灭。配合物**1**对水溶液中亚甲基蓝染料表现出良好的特异性吸附效果,作用49 min后吸附率可达81%。

关键词: 铜(II)配合物; (+)-二对甲基苯甲酰- D -酒石酸; 晶体结构; 荧光; 染料吸附

中图分类号: O614.121 文献标识码: A 文章编号: 1001-4861(2022)06-1112-09

DOI: 10.11862/CJIC.2022.109

Structure, Thermostability, Fluorescence, and Dye Adsorption Properties of a Copper(II) Coordination Polymer Based on (+)-Di-*p*-toluoyl-*D*-tartaric Acid

ZHENG Huan CHU Yan-Xiao FENG Si-Si* YUAN Cai-Xia*

(Institute of Molecular Science, Key Laboratory of Chemical Biology and Molecular Engineering of
Ministry of Education, Shanxi University, Taiyuan 030006, China)

Abstract: A coordination polymer, formulated as $[[\text{Cu}(\text{HDTTA})_2(\text{DMF})(\text{H}_2\text{O})]\cdot\text{DMF}\cdot\text{H}_2\text{O}]_n$ (**1**) (D - $\text{H}_2\text{DTTA}=(+)$ -di-*p*-toluoyl- D -tartaric acid, $\text{DMF}=N,N$ -dimethylformamide), has been synthesized. Its structure was characterized by IR spectrum, elemental analysis, X-ray single-crystal diffraction, and powder X-ray diffraction. Complex **1** features a 1D chain structure along the a -axis and forms a 2D layered structure in the ab plane through weak intermolecular interactions. The thermal decomposition process of **1** included the loss of solvent molecules below 197 °C and follow-up decomposition of the main structure. Under the excitation of 300 nm, the fluorescence of the ligand was quenched by the coordinated Cu^{2+} cation. In addition, complex **1** exhibited a good and specific adsorption effect on methylene blue dye in an aqueous solution with an adsorption rate of 81% after 49 min. CCDC: 2122082.

Keywords: copper(II) complex; (+)-di-*p*-toluoyl- D -tartaric acid; crystal structure; fluorescence; dye adsorption

0 Introduction

Coordination polymers (CPs) are structures connected by inorganic metal clusters or metal cations and organic ligands, with periodic coordination entities

extending in 1D, 2D, or 3D space^[1]. As a new kind of inorganic-organic hybrid material, CPs have a wide range of applications in adsorption and separation^[2-4], catalysis^[5,6], optical materials^[7-8], and magnetism^[9], etc.

In recent decades, organic dyes are widely used,

收稿日期:2021-12-01。收修改稿日期:2022-03-13。

山西省1331工程重点创新研究团队、山西省自然科学基金(No.201901D111014)和山西省归国留学基金(No.2020-001)资助。

*通信联系人。E-mail: ssfeng@sxu.edu.cn, cxyuan@sxu.edu.cn

not only in papermaking, textile printing, and dyeing but also in plastic and cosmetic industries^[10-11]. These industries produced a large amount of industrial wastewater in the production process and then discharged it into the natural water body, which poses a serious threat to the environment and human health^[12-14]. So environmental protection has become the focus of scientists all over the world^[15]. Common water treatment methods include biological treatment^[15-16], membrane filtration^[17-18], coagulation^[19], ion exchange^[20], and photocatalytic degradation^[21-22], *etc.* However, these methods are costly and complicated and may produce toxic side effects. Adsorption, as one of the simplest, most effective, and most feasible methods, has been widely concerned in environmental water treatment in recent years^[16-23]. Nevertheless, finding effective, reusable, economically viable materials with high adsorption capacity remains a challenge^[18]. CPs, which exhibit high specific surface area, rich and diverse structures, adjustable pore sizes and shapes, and can interact with dye molecules through hydrogen bonding, electrostatic and π - π interactions, have been one of the ideal substitutes for the adsorption of organic dyes^[24-26].

Now, it is still a challenge to accurately predict the structures of CPs^[27], because the synthesis could be affected by many factors, such as metals, organic ligands, solvents, ratios of metal to ligand, temperature, and pH value^[28-31]. Among them, the selection of an appropriate organic ligand is one of the important factors in the synthesis of CPs. In this study, we focus on a tartaric acid derivative (+)-di-*p*-toluoyl-*D*-tartaric acid (*D*-H₂DTTA) for the following reasons: (a) the carboxyl groups in the ligand can be completely or partially deprotonated to form different coordination patterns, which contributes to the formation of versatile CPs; (b) the aromatic groups contain π electrons, which is con-

ducive to charge conduction and can help to obtain materials with good optical, electrical, and magnetic properties^[32].

In this paper, the copper complex $\{[\text{Cu}(\text{HDTTA})_2(\text{DMF})(\text{H}_2\text{O})] \cdot \text{DMF} \cdot \text{H}_2\text{O}\}_n$ (**1**) (DMF=*N,N*-dimethylformamide) was successfully synthesized by solvent evaporation method with transition metal copper cation and *D*-H₂DTTA. The structure of complex **1** was characterized by IR spectrum, elemental analysis (EA), X-ray single-crystal diffraction, and powder X-ray diffraction (PXRD). Moreover, thermostability, fluorescence, and dye adsorption properties of complex **1** were also studied.

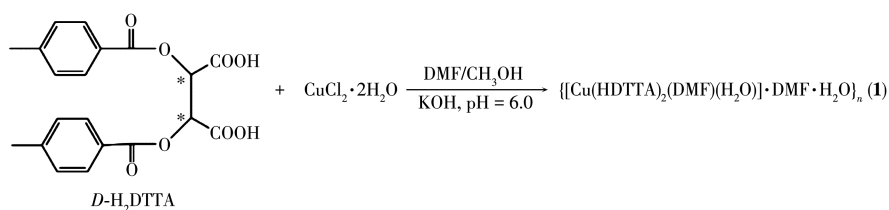
1 Experimental

1.1 Materials and measurements

The *D*-H₂DTTA ligand was bought from TCI (Shanghai) Development Co., Ltd. and used directly without further purification. All solvents and other reagents were of standard commercial grade and used directly without further purification. The sample for EA was dried under a vacuum and the test was performed with a CHN - O - Rapid instrument. IR spectra were obtained on KBr pellets with a BRUKER TENSOR27 spectrometer. PXRD patterns were collected on a Bruker D8 Advance X-ray diffractometer employing Cu $K\alpha$ radiation ($\lambda=0.15418$ nm) with a 2θ range of 5° - 50° . The operating voltage and current were 40 kV and 25 mA, respectively. Thermogravimetric analysis (TGA) was performed on a Dupont thermal analyzer under a nitrogen atmosphere with a heating rate of $10^\circ\text{C} \cdot \text{min}^{-1}$. Fluorescence analyses were performed on a Fluoromax-4 spectrofluorometer with a xenon arc lamp as the light source. The UV - Vis spectra were obtained with a JASCO V-570 spectrophotometer.

1.2 Preparations of complex 1

As shown in Scheme 1, *D*-H₂DTTA (1.25 mmol,



Scheme 1 Synthesis of complex **1**

0.483 0 g) was dissolved in a mixture of 10 mL DMF and 15 mL methanol, then 5 mL methanol solution of $\text{CuCl}_2 \cdot 2\text{H}_2\text{O}$ (0.65 mmol, 0.110 8 g) was added. The mixture was stirred at room temperature for 10 min, then KOH solution ($0.2 \text{ mol} \cdot \text{L}^{-1}$, 5 mL) was added slowly. The mixture was stirred at room temperature for 8 h. After the mixture was filtered, the blue filtrate was placed in a $4 \text{ }^\circ\text{C}$ refrigerator. Two weeks later, blue bulk single crystals of **1** suitable for the X-ray diffraction test were obtained with a yield of 35%. EA for $\text{C}_{46}\text{H}_{52}\text{N}_2\text{O}_{20}\text{Cu}$ (%): C 54.36 (Calcd. 54.31); N 2.76 (Calcd. 2.68); H 5.16 (Calcd. 5.12). IR (KBr, cm^{-1}): 3 570w, 2 938w, 1 720s, 1 653s, 1 611s, 1 509w, 1 416m, 1 372m, 1 331m, 1 267s, 1 178s, 1 112s, 842w, 753m, 697m, 603w, 519w, 486w, 451w.

1.3 X-ray crystallography

X-ray single-crystal diffraction data for **1** were collected on a Bruker SMART APEX II diffractometer

with a CCD area detector and Mo $K\alpha$ radiation $\lambda = 0.071\ 073 \text{ nm}$ at 298(2) K. Multi-scan program SADABS was used for absorption correction^[33]. The structure was solved by the direct method and refined by the full-matrix least-squares method on F^2 using the SHELXTL-2014^[34]. All the non-hydrogen atoms were refined anisotropically. Hydrogen atoms attached to C atoms were placed geometrically and refined by using a riding model approximation, with C—H lengths of 0.093 - 0.098 nm. Hydrogen atoms in hydroxyl and water molecules were located from different Fourier maps and refined using their global U_{iso} value with an O—H length of 0.082 nm. A summary of the crystallographic data and structure refinements for complex **1** is provided in Table 1. Selected bond lengths and angles for **1** are provided in Table 2.

CCDC: 2122082.

Table 1 Crystal data and structure refinements for complex **1**

Parameter	1	Parameter	1
Formula	$\text{C}_{46}\text{H}_{52}\text{N}_2\text{O}_{20}\text{Cu}$	$F(000)$	1 062
Formula weight	1 016.43	$D_c / (\text{Mg} \cdot \text{m}^{-3})$	1.356
Crystal system	Monoclinic	μ / mm^{-1}	0.52
Space group	$P2_1$	Flack	0.039(15)
a / nm	0.745 39(7)	Reflection collected	15 201
b / nm	2.521 9(2)	Independent reflection	9 524
c / nm	1.327 51(13)	R_{int}	0.031
$\beta / (^\circ)$	93.886(3)	GOF	1.139
V / nm^3	2.489 7(4)	$R_1, wR_2 [I > 2\sigma(I)]$	0.046 6, 0.082 0
Z	2	R_1, wR_2 (all data)	0.069 8, 0.088 1

Table 2 Selected bond lengths (nm) and angles ($^\circ$) for **1**

Cu1—O18	0.193 0(3)	Cu1—O17	0.193 9(4)	Cu1—O1	0.194 1(3)
Cu1—O9	0.195 0(3)				
O18—Cu1—O17	172.96(16)	O18—Cu1—O1	90.50(14)	O17—Cu1—O1	88.45(14)
O18—Cu1—O9	88.97(14)	O17—Cu1—O9	92.21(14)	O1—Cu1—O9	178.76(14)

1.4 Dye adsorption

The dye adsorption ability of complex **1** was evaluated by the adsorption of three organic dyes including methyl orange (MO), rhodamine B (RhB), and methylene blue (MB) in an aqueous solution. At room temperature, 1.5 mg complex **1** was added to 15 mL 0.03

$\text{mmol} \cdot \text{L}^{-1}$ dye solution and mechanically stirred continuously. Then, the samples were periodically removed from the reactor and immediately centrifuged to separate any suspended solids. The transparent solution was transferred to a trace cuvette and analyzed by a UV-Vis spectrometer.

2 Results and discussion

2.1 IR spectra

IR spectra of *D*-H₂DTTA and complex **1** were examined at room temperature (Fig. 1). The C=O stretching vibration characteristic absorption peaks at the positions of 1 739 and 1 672 cm⁻¹ for *D*-H₂DTTA were shifted to 1 720 and 1 653 cm⁻¹ for complex **1**, respectively^[35]. At the same time, the characteristic absorption peaks of C—O stretching vibration at 1 250 and 1 115 cm⁻¹ were shifted to 1 267 and 1 112 cm⁻¹, respectively^[36]. The results prove that the carboxyl oxygen atoms in the ligand participate in the coordination to form the complex.

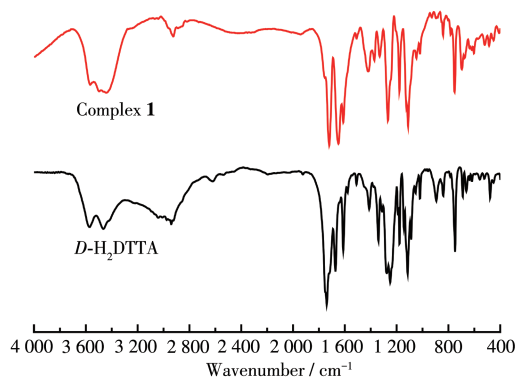


Fig.1 IR spectra of *D*-H₂DTTA and complex **1**

2.2 Crystal structure description

X-ray single-crystal diffraction shows that complex **1** belongs to the monoclinic crystal system and polar *P*2₁ space group. As shown in Fig.2, the asymmetric structure of complex **1** contains a Cu²⁺ ion, two

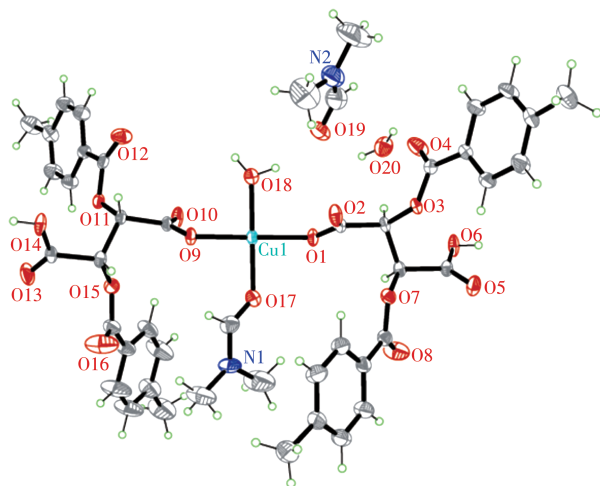
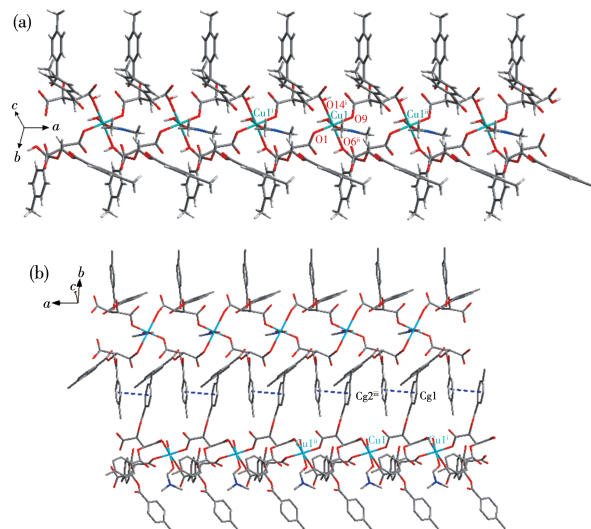


Fig.2 Structure of complex **1** with 30% thermal ellipsoid probability level

HDTTA⁻ ions, a coordinated water molecule, a coordinated DMF molecule, a free water molecule, and a free DMF molecule. The four oxygen atoms coordinated with Cu²⁺ are from the carboxyl oxygen atoms of two HDTTA⁻ ions, and the coordinated DMF and water molecules. The Cu—O bond lengths are in a range of 0.193 1(4)–0.195 0(3) nm, which is similar to those reported Cu²⁺ CPs^[37–38]. Complex **1** forms a 1D chain structure (Fig. 3a) along the *a*-axis with the distance between copper cations of 0.745 4(1) nm, and $\pi \cdots \pi$ weak interaction between Cg1 (the centroid of the C6—C11 ring) and Cg2 (the centroid of the C26—C31 ring) helps complex **1** to form a 2D planar structure in the *ab* plane. The distance between the rings is 0.379 4 nm (Fig.3b).



H atoms have been omitted for clarity; Symmetry codes: ⁱ $x-1, y, z$; ⁱⁱ $x+1, y, z$; ⁱⁱⁱ $-x+2, y+1/2, -z+1$

Fig.3 (a) One-dimensional chain-like structure of complex **1**; (b) Weak $\pi \cdots \pi$ intermolecular interactions in complex **1**

2.3 PXRD pattern and thermal analysis

To verify the phase purity of the complex, a PXRD analysis was performed. The experimental PXRD pattern was consistent with the calculated one based on the X-ray single-crystal data, certifying the high phase purity of the complex (Fig. 4). In order to estimate the thermal stability of **1**, TGA was performed in a range of 25–800 °C (Fig. 5). In the range of 51–80 °C, complex **1** had a weight loss of 3.34%, equivalent to a solvent water molecule and a coordinated

water molecule (Calcd. 3.54%). Then the curve went through a plateau up to 157 °C. In 157-197 °C range, complex **1** lost 7.24% weight, equivalent to a solvent DMF molecule (Calcd. 7.19%), and then, with heating temperature, the framework gradually broke down.

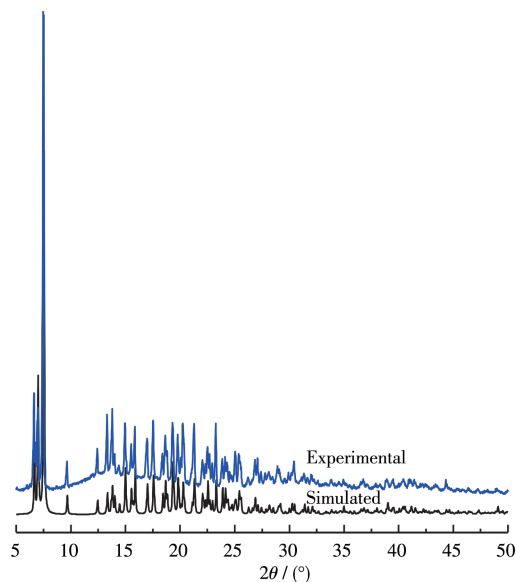


Fig.4 Simulated and experimental PXRD patterns of complex **1**

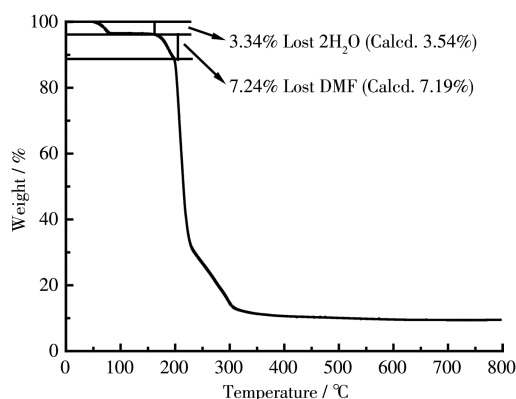


Fig.5 TGA curve of complex **1**

2.4 Fluorescence properties

The solid - state photoluminescent properties of *D*-H₂DTTA and complex **1** were investigated. Fig. 6 shows that when the excitation wavelength was 300 nm, the ligand *D*-H₂DTTA exhibited strong emission peaks at 357 and 680 nm, which are either $\pi^*-\pi$ or $\pi^*-\pi$ transitions of the ligand. Under the same conditions, no fluorescence emission peak was found for complex **1**. Because Cu²⁺ has the 3d⁹ unsaturated electron configuration, there is electron transfer between Cu²⁺ and

ligand, leading to fluorescence quenching of the ligand^[39-40].

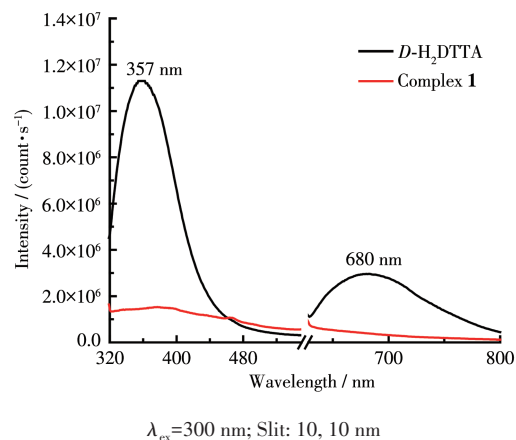


Fig.6 Solid fluorescence emission spectra of *D*-H₂DTTA and **1**

2.5 Dyes adsorption

Three organic dyes, MB, RhB, and MO, were used as the model pollutant in aqueous media to evaluate the adsorption property of **1**. The results showed that complex **1** displayed good specific adsorption ability to MB but little effect on MO and RhB under the same condition. As shown in Fig.7a, the variation of UV-Vis spectra of MB dye solution in the presence of **1** was measured at each 7 min interval. The spectra displayed that the characteristic absorption peak of MB at 665 nm decreased by 81% after 49 min, implying the significant dye removal behavior of **1** for MB from an aqueous solution. Fig.7b shows the variation of MB concentration (c/c_0) with reaction time, where c_0 is the initial concentration of the MB solution, and c is the concentration of the MB solution after the adsorption. Controlled experiments were also performed. Under the same experimental conditions, the concentration of MB remained essentially unchanged after 49 min without the addition of complex **1**, implying that MB was relatively stable in the solution.

The reaction suspension was centrifuged and the MB on the solid surface was washed away with water, and the resulting material was detected by IR (Fig.8). After adsorption, the C=O and C—O stretching vibration characteristic absorption peaks of complex **1** were maintained at the positions of 1 720, 1 267, and 1 112 cm⁻¹, respectively. The results show that the substance

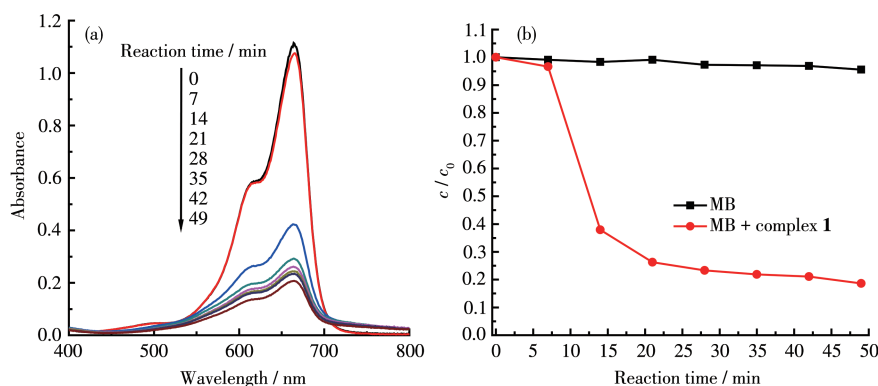


Fig.7 (a) UV-Vis spectra of organic dye MB solution in the presence of complex **1**; (b) Adsorption rate of complex **1** to MB

after adsorption is a mixture of MB and complex **1**, which indicates that complex **1** is a good adsorbent for MB in this experiment. However, when complex **1** was added to the solution of MO and RhB, respectively, the characteristic strength peaks of the dyes had no obvious change (Fig. 9). The difference in adsorption for these three dyes may result from the different sizes and shapes of the dyes. Compared to MO and MB, RhB is a triangular-planar structure and is difficult to be adsorbed by complex **1** due to the large size of RhB.

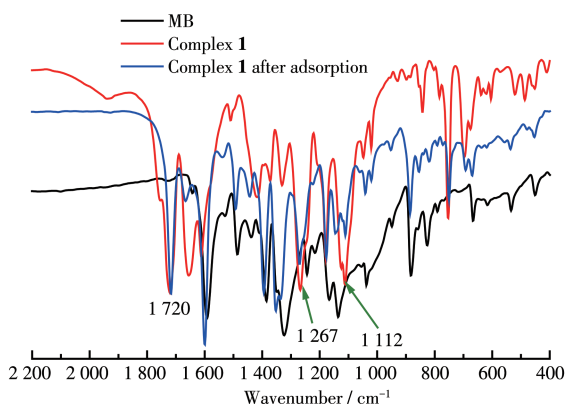


Fig.8 IR spectra of MB and complex **1** before and after the adsorption

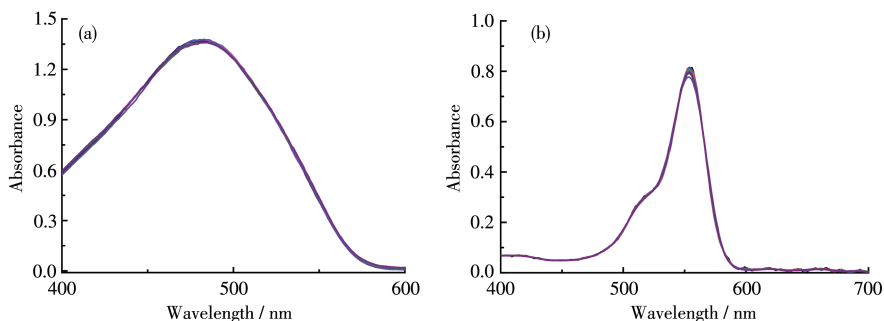


Fig.9 UV-Vis spectra of organic dye (a) MO and (b) RhB solution in the presence of complex **1** within 49 min

Meanwhile, MB and MO with relatively small sizes. The planarity of MB is better than that of MO, which is in favor of $\pi-\pi^*$ stacking interactions between MB and the corresponding adsorbent. So, considering the structure of complex **1**, the specific MB adsorption may be explained to proceed through $\pi-\pi^*$ stacking interactions between MB and the complex^[41-42].

Complex **1** could be recovered by the ultrasonic wave and washed with water and methanol. The recovered sample was used for the next cycle while all other reaction conditions remained unchanged. The performance of complex **1** adsorbed MB did not change significantly in four consecutive cycles, indicating that complex **1** has high stability and can be used for repeated treatment of MB dye (Fig. 10a). PXRD patterns of the recovered sample were basically consistent with the simulated one, indicating that the skeleton of complex **1** has not collapsed after recycling (Fig. 10b).

In order to exclude the influence of other dyes on complex **1**, an anti-interference experiment was explored with MO and RhB dyes mixing with MB, respectively (Fig. 11). The UV-Vis spectra showed that

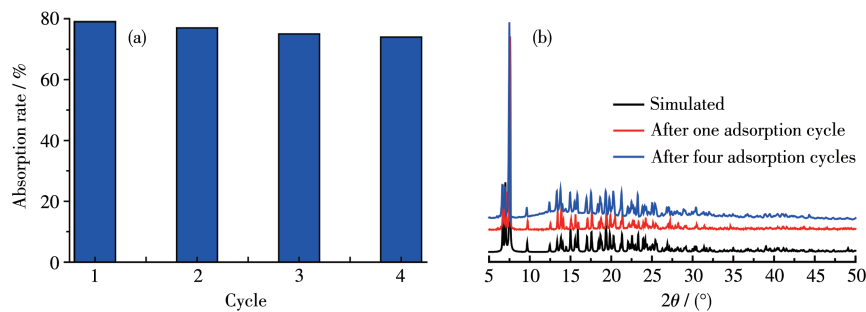


Fig.10 (a) Reusability of complex **1** for adsorption of MB; (b) PXRD patterns of complex **1** after one and four adsorption cycles, respectively

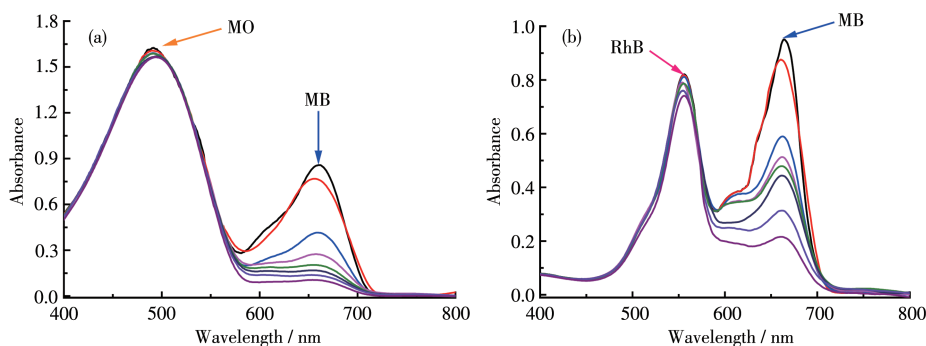


Fig.11 UV-Vis spectra of (a) MO and MB, (b) RhB and MB solution in the presence of complex **1** within 49 min

the MO and RhB dyes had little effect on the adsorption of complex **1** to MB, which proved that complex **1** had selective adsorption on MB. Based on the above experimental investigation, the results indicate that **1** can be used as the potential adsorbent for MB dye molecules.

3 Conclusions

We successfully synthesized a new coordination polymer **1** from $\text{CuCl}_2 \cdot 2\text{H}_2\text{O}$ and $D\text{-H}_2\text{DTTA}$ by solvent volatilization. The structure of complex **1** was determined by X-ray single-crystal diffraction, infrared, elemental analysis, and PXRD characterization. The thermal analysis experiment proved that the main structure of **1** could be maintained up to $197\text{ }^\circ\text{C}$. The fluorescence analysis shows that the fluorescence quenching of complex **1** occurred compared to the ligand because of the introduction of copper cations. The adsorption experiments show that complex **1** has a good and specific adsorption effect on methylene blue dye and can be used as an adsorbent for methylene blue dye.

References:

- [1] 卜显和. 配位聚合物化学. 北京: 科学出版社, 2019.
- [2] Paiman S H, Rahman M A, Uchikoshi T, Abdullah N, Othman D H M, Jaafar J, Abas K H, Ismail A F. Functionalization Effect of Fe-Type MOF for Methylene Blue Adsorption. *J. Saudi Chem. Soc.*, 2020, 24:896-905
- [3] Jie D, Zou G L. A Novel Microporous Zinc(II) Metal-Organic Framework with Highly Selectivity Adsorption of CO_2 over CH_4 . *Inorg. Chem. Commun.*, 2016, 69:20-23
- [4] Zhang L, Yang W B, Wu X Y. A Polyhedron-Based Cobalt-Organic Framework for Gas Adsorption and Separation. *Inorg. Chem. Commun.*, 2016, 67:10-13
- [5] Leus K, Bogaerts T, Decker J D, Depauw H, Hendrickx K, Vrielandt H, Speybroeck V, Voort P V D. Systematic Study of the Chemical and Hydrothermal Stability of Selected "Stable" Metal Organic Frameworks. *Microporous Mesoporous Mater.*, 2016, 226:110-116
- [6] He H B, Li R, Yang Z Y, Chai L Y, Jin L F, Alhassan I S, Ren L L, Wng H Y, Huang L. Preparation of MOFs and MOFs Derived Materials and Their Catalytic Application in Air Pollution: A Review. *Catal. Today*, 2021, 375:10-29
- [7] Zhu J Y, Xia T F, Cui Y J, Yang Y, Qian G D. A Turn-On MOF-Based Luminescent Sensor for Highly Selective Detection of Glutathione. *J. Solid State Chem.*, 2019, 270:317-323
- [8] Zhu M, Li M T, Zhao L, Shao K Z, Su Z M. Metal-Organic Frameworks (The Original is "Fameworks") Based on Multi-carboxylate Ligands with Threefold Symmetries and Luminescence Properties. *Inorg. Chem. Commun.*, 2017, 79:69-73
- [9] Pandey S, Demaske B, Ejegbavwo O A. Electronic Structures and

- Magnetism of Zr-, Th-, and U-Based Metal-Organic Frameworks (MOFs) by Density Functional Theory. *Comput. Mater. Sci.*, **2020**,**184**: 109903
- [10]Donkadokula N Y, Kola A K, Naz I, Saroj D. A Review on Advanced Physico-Chemical and Biological Textile Dye Wastewater Treatment Techniques. *Rev. Environ. Sci. Biotechnol.*, **2020**,**19**:543-560
- [11]Harvey P J, Handley H K, Taylor M P. Identification of the Sources of Metal (Lead) Contamination in Drinking Waters in North-Eastern Tasmania Using Lead Isotopic Compositions. *Environ. Sci. Pollut. Res.*, **2015**,**22**:12276-12288
- [12]Sansuk S, Srijaranai S, Srijaranai S. A New Approach for Removing Anionic Organic Dyes from Wastewater Based on Electrostatically Driven Assembly. *Environ. Sci. Technol.*, **2016**,**50**:6477-6484
- [13]de Luna L A V, da Silva T H G, Nogueira P R F, Kummrow F, Umbuzeiro G A. Aquatic Toxicity of Dyes before and after Photo-Fenton Treatment. *J. Hazard. Mater.*, **2014**,**276**:332-338
- [14]Mathieu-Denoncourt J, Martyniuk C J, de Solla S R, Balakrishnan V K, Langlois V S. Sediment Contaminated with the Azo Dye Disperse Yellow 7 Alters Cellular Stress- and Androgen-Related Transcription in *Silurana tropicalis* Larvae. *Environ. Sci. Technol.*, **2014**,**48**: 2952-2961
- [15]Parasuraman D, Serpe M J. Poly(*N*-isopropylacrylamide) Microgels for Organic Dye Removal from Water. *ACS Appl. Mater. Interfaces*, **2011**,**3**:2732-2737
- [16]Ceretta M B, Necessian D, Wolski E A. Current Trends on Role of Biological Treatment in Integrated Treatment Technologies of Textile Wastewater. *Front. Microbiol.*, **2021**,**12**:651025
- [17]Agnieszka K R, Nghiem L D, Teofil J. Functionalized Materials as a Versatile Platform for Enzyme Immobilization in Wastewater Treatment. *Curr. Pollut. Rep.*, **2021**,**7**:263-276
- [18]Kumar S P, Gayathri R, Senthil R B. A Review on Adsorptive Separation of Toxic Metals from Aquatic System Using Biochar Produced from Agro-Waste. *Chemosphere*, **2021**,**285**:131438
- [19]Chen B Y, Jiang J Y, Yang X, Zhang X R, Westerhoff P. Roles and Knowledge Gaps of Point-of-Use Technologies for Mitigating Health Risks from Disinfection Byproducts in Tap Water: A Critical Review. *Water Res.*, **2021**,**200**:117265
- [20]Zhu G C, Bian Y N, Hursthouse A S, Xu S N, Xiong N N, Wan P. The Role of Magnetic MOFs Nanoparticles in Enhanced Iron Coagulation of Aquatic Dissolved Organic Matter. *Chemosphere*, **2020**,**247**: 125921
- [21]Ridha N J, Mohamad Alosfur F K, Kadhim H B A, Ahmed L M. Synthesis of Ag Decorated TiO₂ Nanoneedles for Photocatalytic Degradation of Methylene Blue Dye. *Mater. Res. Express*, **2021**,**8**:125013
- [22]Hussain T, Hussain M, Hussain S, Kaseem M. Microwave-Assisted Synthesis of NiTe₂ Photocatalyst as a Facile and Scalable Approach for Energy-Efficient Photocatalysis and Detoxification of Harmful Organic Dyes. *Sep. Purif. Technol.*, **2022**,**282**:120025
- [23]Li L, Yang M, Lu Q, Zhu W K, MaH Q, Dai L C. Oxygen-Rich Biochar from Torrefaction: A Versatile Adsorbent for Water Pollution Control. *Bioresour. Technol.*, **2019**,**294**:122142
- [24]Chen Y B, Tang J L, Wang S X, Zhang L B. High Selectivity and Reusability of Coordination Polymer Adsorbents: Synthesis, Adsorption Properties and Activation Energy. *Microporous Mesoporous Mater.*, **2021**,**324**:111309
- [25]Lai Z Z, Yang X, Qin L, An J L, Wang Z, Sun X, Zhang M D. Synthesis, Dye Adsorption, and Fluorescence Sensing of Antibiotics of a Zinc-Based Coordination Polymer. *J. Solid State Chem.*, **2021**,**300**: 122278
- [26]Lippi M, Cametti M. Highly Dynamic 1D Coordination Polymers for Adsorption and Separation Applications. *Coord. Chem. Rev.*, **2021**, **430**:213661
- [27]Tranchemontagne D J, O'Keeffe M, Yaghi O M. Reticular Chemistry of Metal-Organic Polyhedra. *Angew. Chem. Int. Ed.*, **2008**,**47**:5136-5147
- [28]Hu T P, Wang X X, Xue Z J, Zhang X. Structural Control and Magnetic Properties of Three Co(II) Coordination Polymers Based on 6-(3,5-Dicarboxyphenyl)nicotinic Acid. *Polyhedron*, **2017**,**127**:449-457
- [29]Yue Q Y, Lu Y M, Chuan F X, Yuan D, Chen D Y, Yang G W, Li Q Y. Synthesis, Crystal Structure, Luminescence and Thermal Behavior of a New Energetic Zinc(II) Compound. *Inorg. Chem. Commun.*, **2016**,**68**:68-71
- [30]Xie F T, Bie H Y, Duan L M, Li G H, Zhang X, Xu J Q. Self-Assembly of Silver Polymers Based on Flexible Isonicotinate Ligand at Different pH Values: Syntheses, Structures and Photoluminescent Properties. *J. Solid State Chem.*, **2005**,**178**:2858-2866
- [31]Manna K, Zhang T, Carboni M, Abney C W, Lin W B. Salicylaldehyde-Based Metal-Organic Framework Enabling Highly Active Olefin Hydrogenation with Iron and Cobalt Catalysts. *J. Am. Chem. Soc.*, **2014**,**136**:13182-13185
- [32]Zhang J, Gao L L, Wang Y, Zhai L J, Wang X Q, Fan L M, Hu T P. Two Trinuclear Cluster-Based 3D Interpenetrated Metal-Organic Frameworks with Selective Adsorption and Antiferromagnetic Properties. *J. Solid State Chem.*, **2019**,**271**:303-308
- [33]Sheldrick G M. A Short History of SHELX. *Acta Crystallogr. Sect. A*, **2008**,**A64**:112-122
- [34]Sheldrick G M. Crystal Structure Refinement with SHELXL. *Acta Crystallogr. Sect. C*, **2015**,**C71**:3-8
- [35]Ma X L, Wang Z X, He X, Shao M, Li M X. 2D Double-Layered Dibenzoyl-Tartrate Chiral Coordination Polymer Containing [Mn₄L₂(bpp)₄] Tetrahedral Cage. *Inorg. Chem. Commun.*, **2018**,**92**:131-135
- [36]张雪, 孙媛媛, 冯思思, 袁彩霞. 基于二苯甲酰酒石酸构筑的钴、镍配合物的合成、结构、荧光及磁性. *无机化学学报*, **2021**,**37**(12):2279-2288
- ZHANG X, SUN Y Y, FENG S S, YUAN C X. Synthesis, Structures, Luminescence and Magnetic Properties of Co(II) and Ni(II) Coordination Compounds Based on Dibenzoyl-Tartaric Acid. *Chinese J. Inorg. Chem.*, **2021**,**37**(12):2279-2288
- [37]Li D, Lv N, Yu J K, Qiao Y, Xue X X, Li H J, Che G B. Synthesis, Crystal Structure and Highly Sensitive Detection Property of a Fluorescent Copper Coordination Polymer. *J. Mol. Struct.*, **2021**, **1236**: 130347

- [38] Liu C X, Cui J, Wang Y F, Zhang M J. A Novel Two-Dimensional Metal-Organic Framework as a Recyclable Heterogeneous Catalyst for the Dehydrogenative Oxidation of Alcohol and the *N*-Arylation of Azole Compounds. *RSC Adv.*, **2021**,**11**:11739-11744
- [39] Feng S S, Lv H G, Li Z P, Feng G Q, Lu L P, Zhu M L. The First Example of Rhombic Dodecahedral CuBr Clusters in a Novel Mixed-Valence Cu(I , II)-Benzimidazole Complex. *CrystEngComm*, **2012**, **14**:98-102
- [40] He H M, Sun F X, Su H M, Jia J T, Li Q, Zhu G S. Syntheses, Structures and Luminescence Properties of Three Metal-Organic Frameworks Based on 5-(4-(2*H*-Tetrazol-5-yl)phenoxy)isophthalic Acid. *CrystEngComm*, **2014**,**3**:339-343
- [41] Liu Z Q, Zhao Y, Wang P, Kang Y S, Azam M, Al-Resayes S, Liu X H, Lu Y Q, Sun Q Y. Fluorescent Sensing and Selective Adsorption Properties of Metal-Organic Frameworks with Mixed Tricarboxylate and 1*H*-Imidazol-4-yl-Containing Ligands. *Dalton Trans.*, **2017**,**46**: 9022-9029
- [42] Akhtar M N, Mantasha I, Shahid M, AlDamen M A, Khalid M, Akram M. Cationic Dye Adsorption and Separation at Discrete Molecular Level: First Example of an Iron Cluster with Rapid and Selective Adsorption of Methylene Blue from Aqueous System. *New J. Chem.*, **2021**,**45**:1415-1422